



## **Supplemental Material to:**

**Yangqing Xu, Junying Yuan and Marta M. Lipinski**

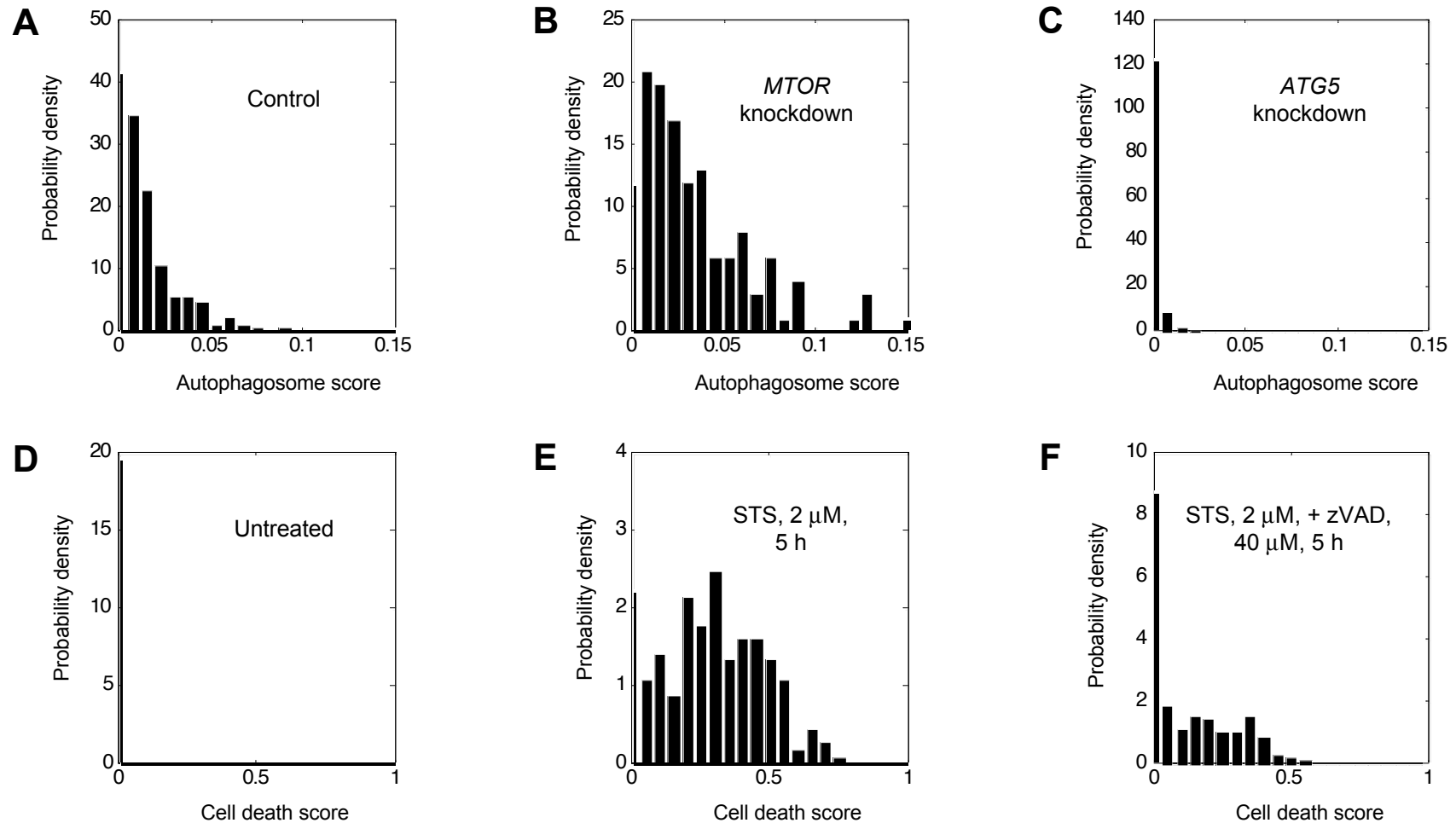
**Live imaging and single-cell analysis reveal differential dynamics of autophagy and apoptosis**

**Autophagy 2013; 9(9)**

**<http://dx.doi.org/10.4161/auto.25080>**

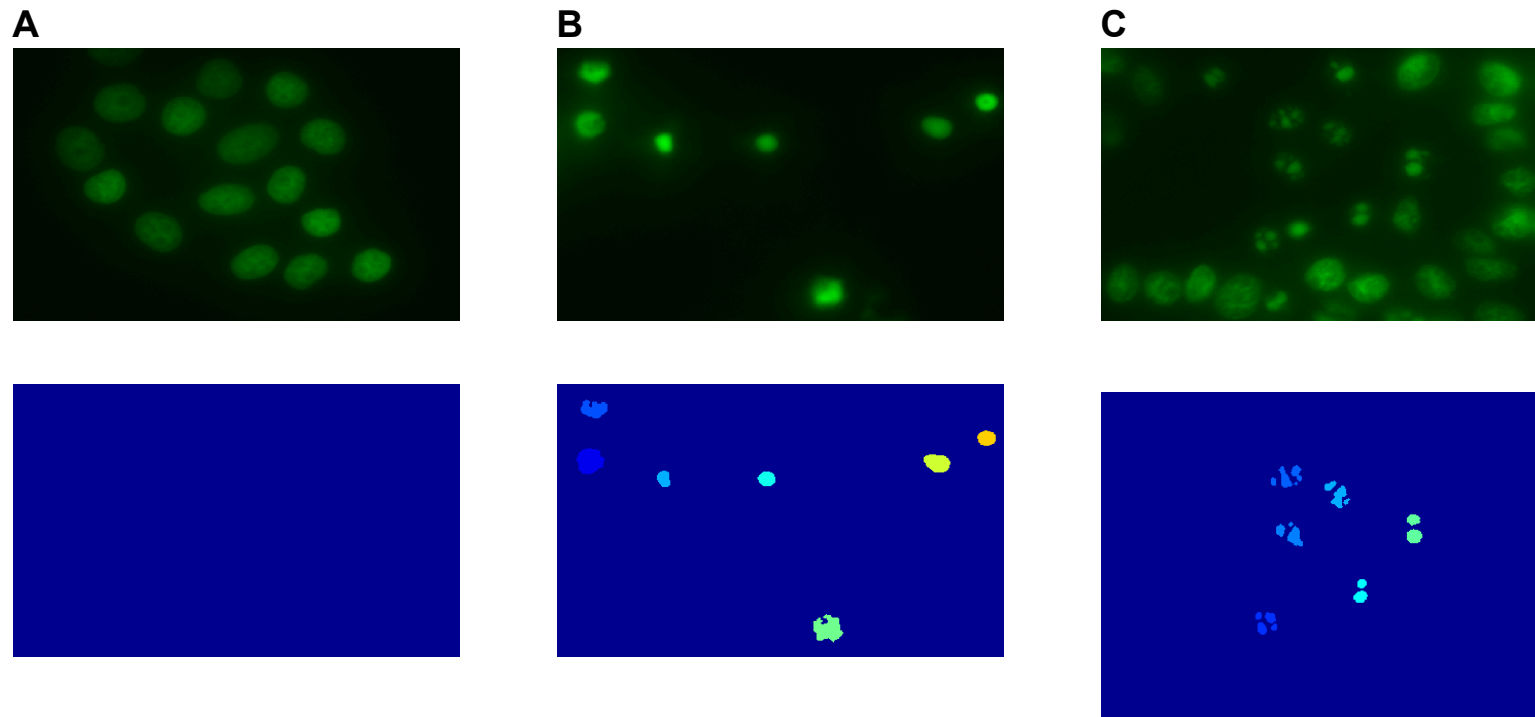
**[www.landesbioscience.com/journals/autophagy/article/25080](http://www.landesbioscience.com/journals/autophagy/article/25080)**

## Figure S1. Validation of Image Analysis



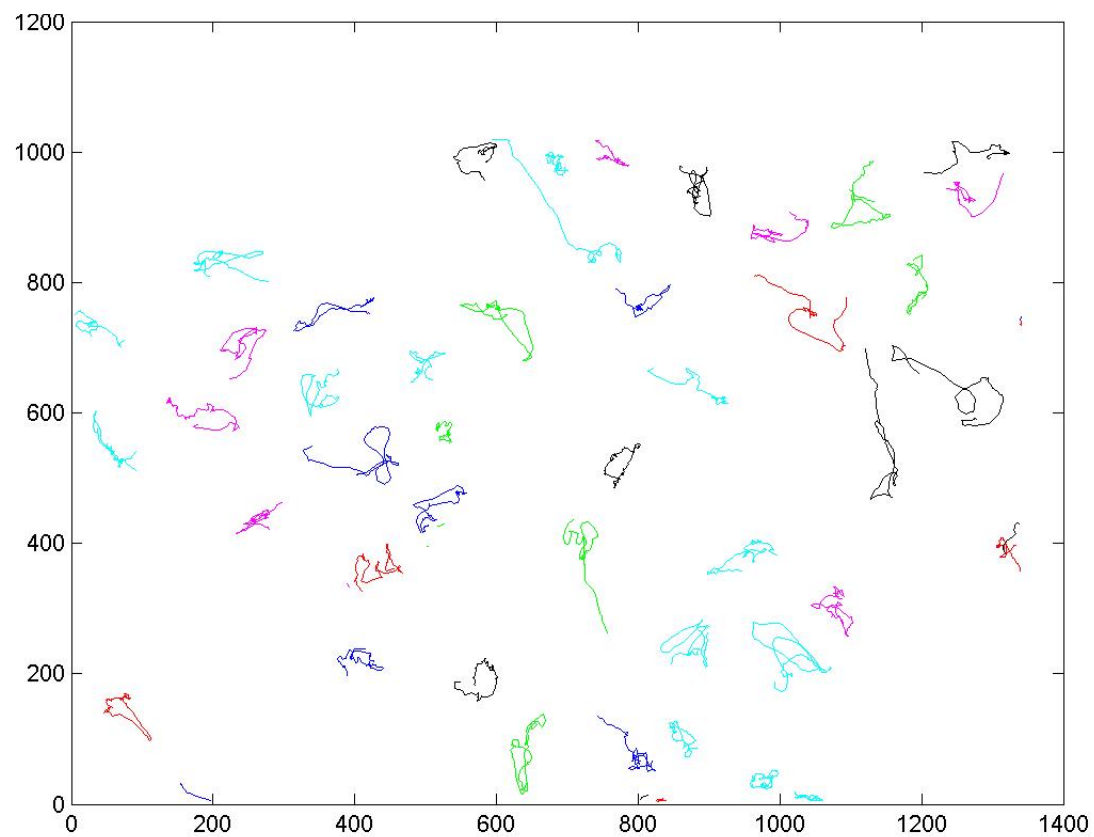
**Figure S1.** Validation of image analysis and puncta score measurements. Autophagosome score was measured in cells transfected with (A) non-targeting siRNA control, (B) siRNA against *MTOR*, or (C) siRNA against *ATG5*. Cell death score was measured in cells that were (D) untreated, (E) treated with 2  $\mu$ M staurosporine (STS) for 5 h, or (F) 2  $\mu$ M STS + 40  $\mu$ M zVAD for 5 h.

## Figure S2. Apoptosis and mitotic arrest can be distinguished by image analysis



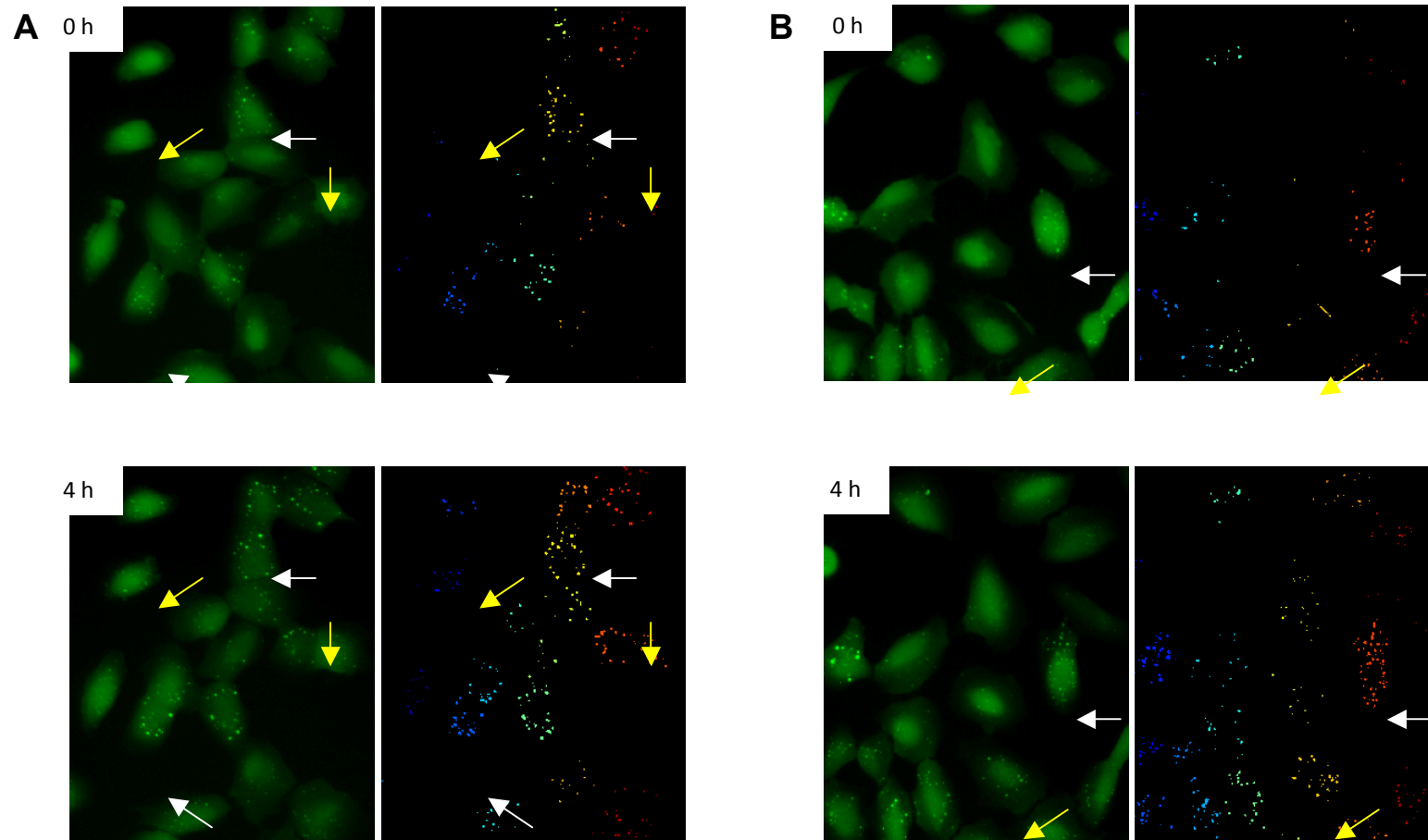
**Figure S2.** Detection of mitotic arrest and apoptosis in HeLa H2B-GFP cells. Images of H2B-GFP are shown in top row, and the corresponding segmented images are in the bottom row. **(A)** Normal cells, where no puncta are detected. **(B)** Cells arrested in mitosis by 300 nM nocodazole for 36 h. Each nucleus is identified as a single particle. **(C)** Apoptosis induced by 2.5  $\mu$ M STS for 10 h. In this case, multiple small puncta are detected in each apoptotic nucleus. The number of puncta is labeled next to each corresponding nucleus.

Figure S3. Live cell trajectories generated by automated cell tracking



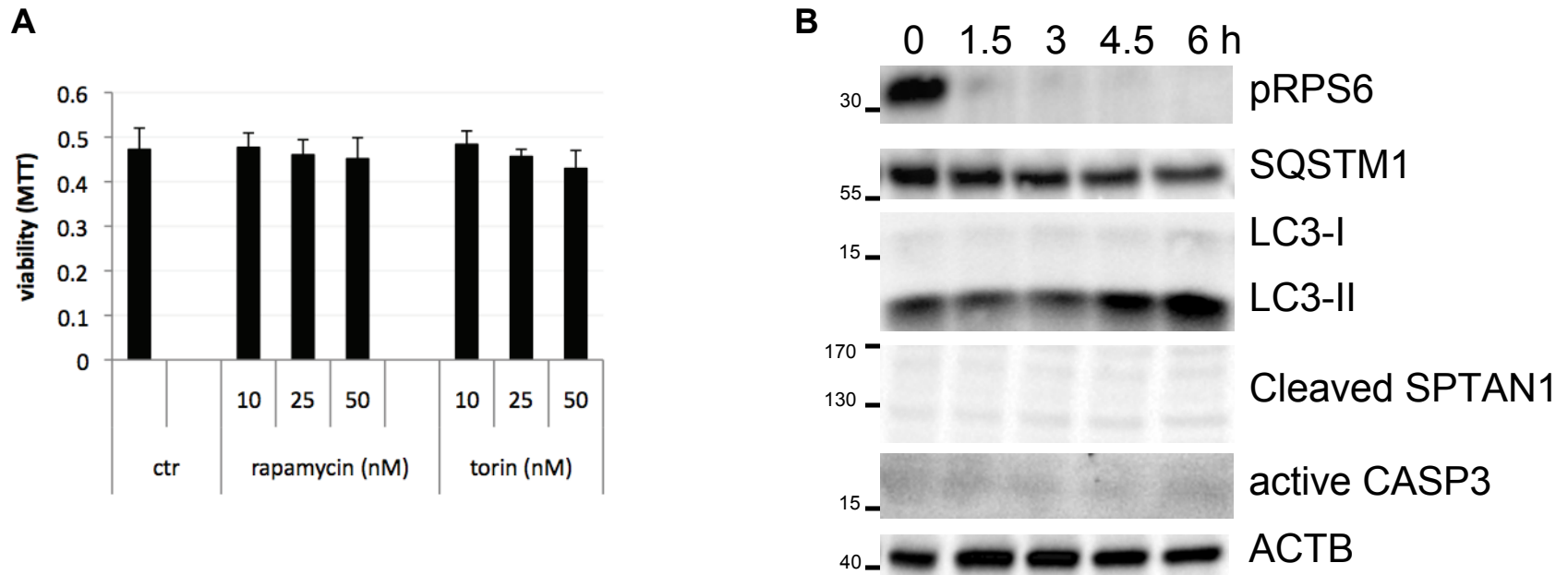
**Figure S3.** Typical cell trajectories obtained by automated cell tracking. Coordinates in X-axis and Y-axis are pixels.

## Figure S4. Starvation leads to increased levels of autophagy in H4 cells



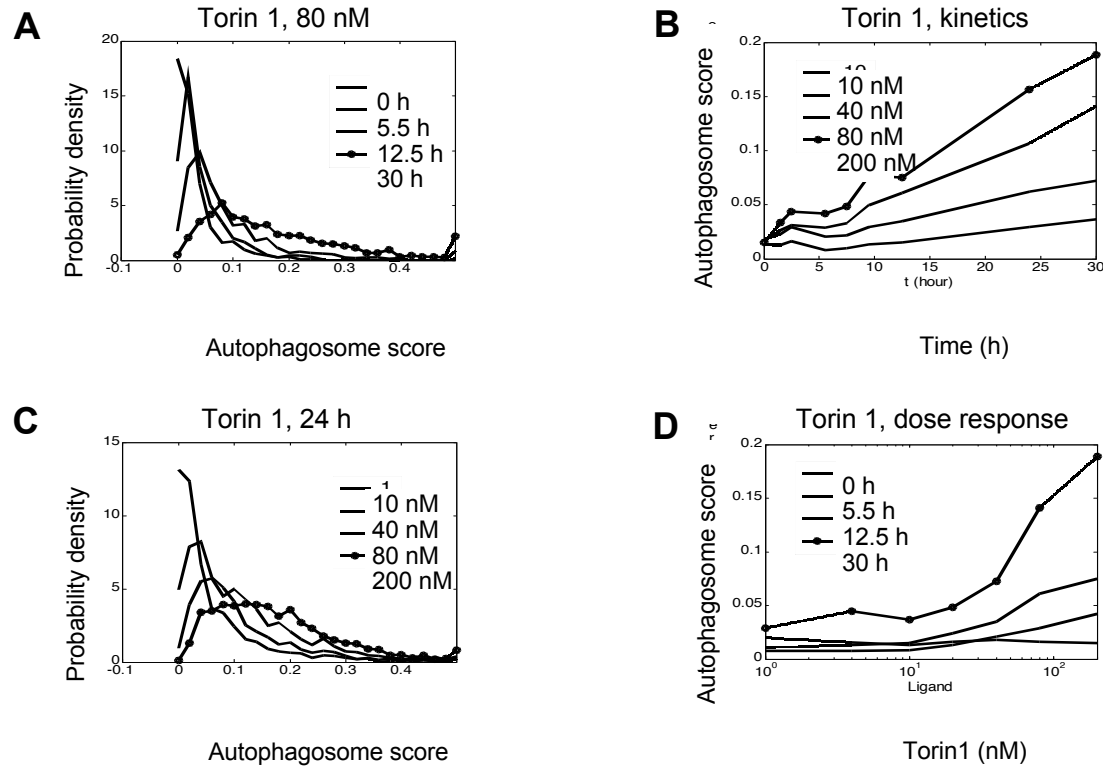
**Figure S4.** Starvation-induced autophagy in H4 cells. **(A)** Serum starvation. **(B)** Glucose starvation. Yellow arrows point to cells with few puncta at time 0 h, and white arrows point to cells with relatively more puncta at time 0 h. Note the increase of puncta number and intensity at 4 h.

# Figure S5. Inhibition of MTOR leads to induction of autophagy but not apoptosis.



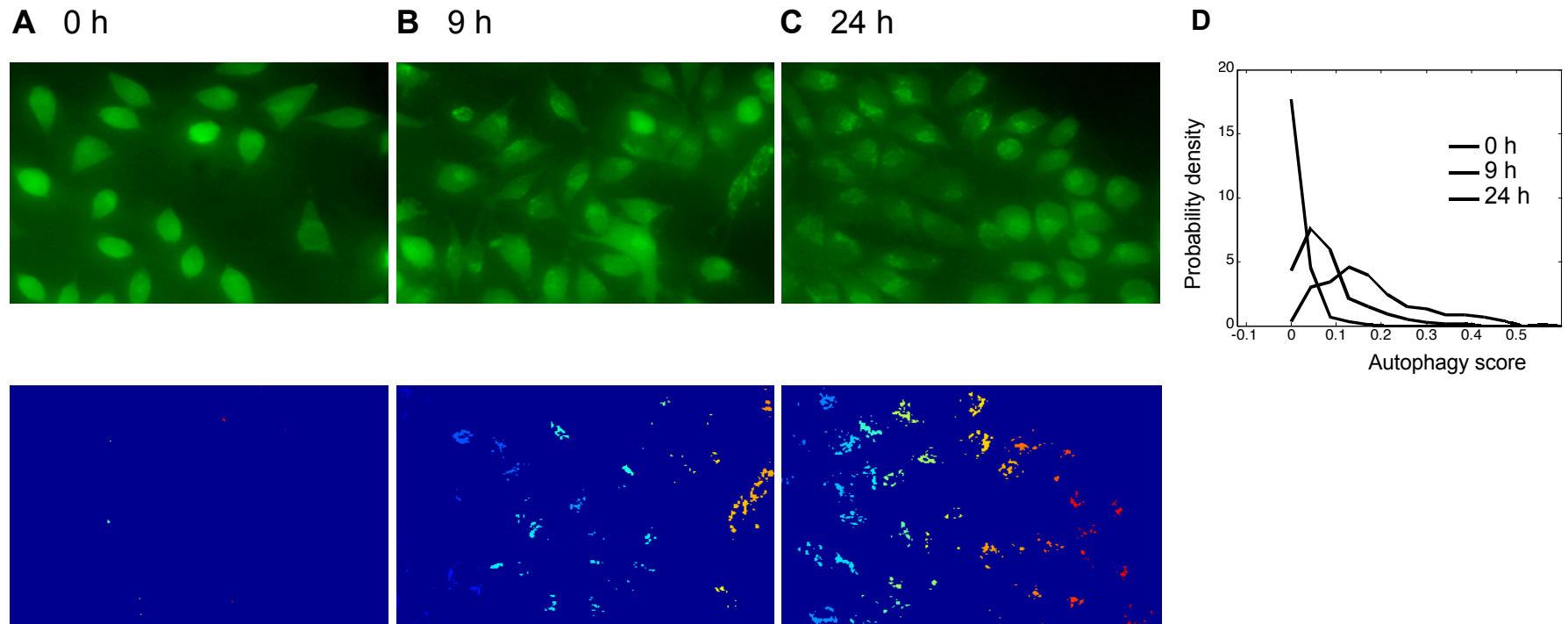
**Figure S5.** Inhibition of MTOR leads to induction of autophagy but not apoptosis. **(A)** Treatment with either rapamycin or Torin 1 for 5 h failed to decrease H4 cell viability as assessed by MTT assay. **(B)** Treatment of H4 cells with 50 nM rapamycin induced autophagy (accumulation of LC3-II and decreased levels of SQSTM1) but no cell death (no increase in cleaved SPTAN1 or active CASP3). Cells were treated with bafilomycin A<sub>1</sub> (Baf) for 6 h prior to lysis.

## Figure S6. Torin 1-induced autophagy in H4 cells



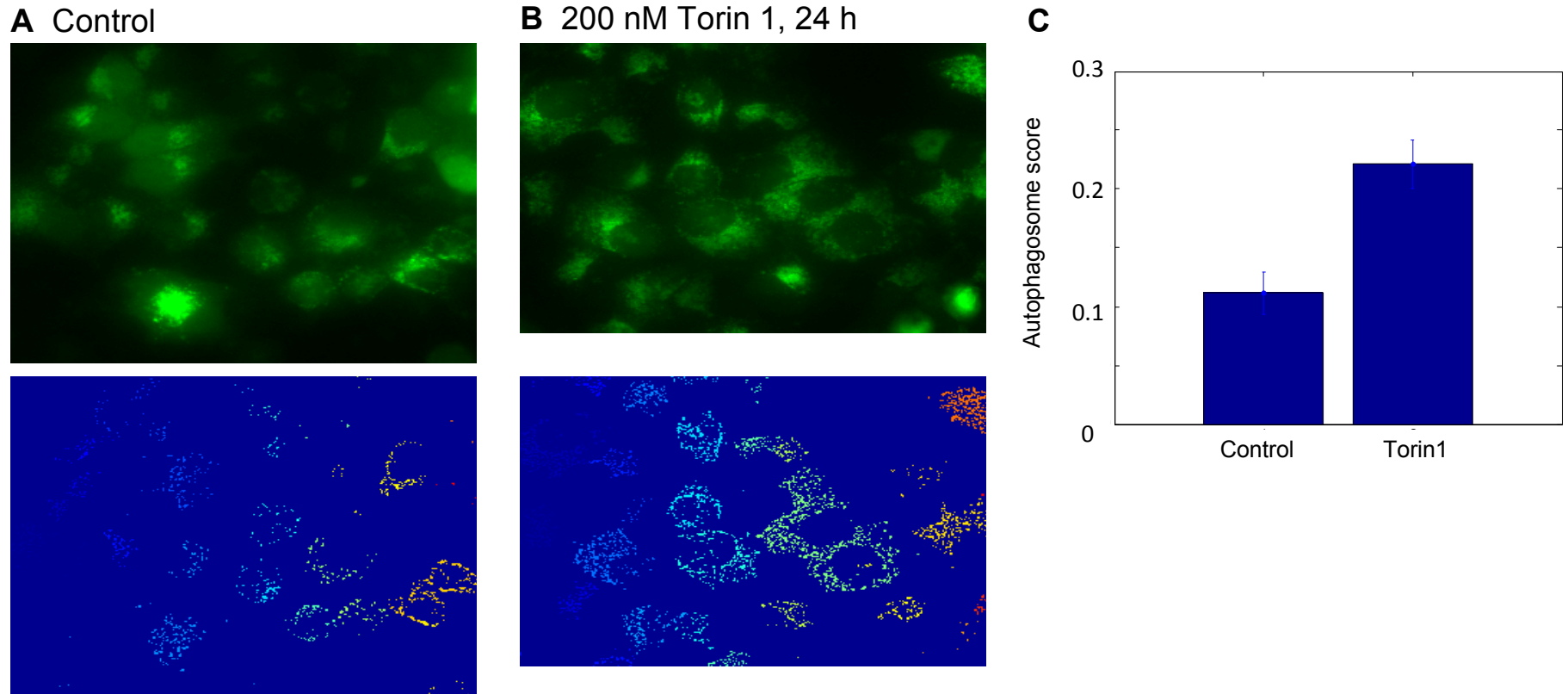
**Figure S6.** Torin 1-induced autophagy in H4 cells. **(A)** Kinetics of autophagy distributions after 80 nM of Torin 1 treatment. **(B)** Average kinetics after Torin 1 treatment at the indicated concentrations. **(C)** Dose-response of autophagy distributions after 24 h of Torin 1 treatment. **(D)** Average dose-response after Torin 1 treatment at the indicated time points.

## Figure S7. Torin 1-induced autophagy in L929 cells



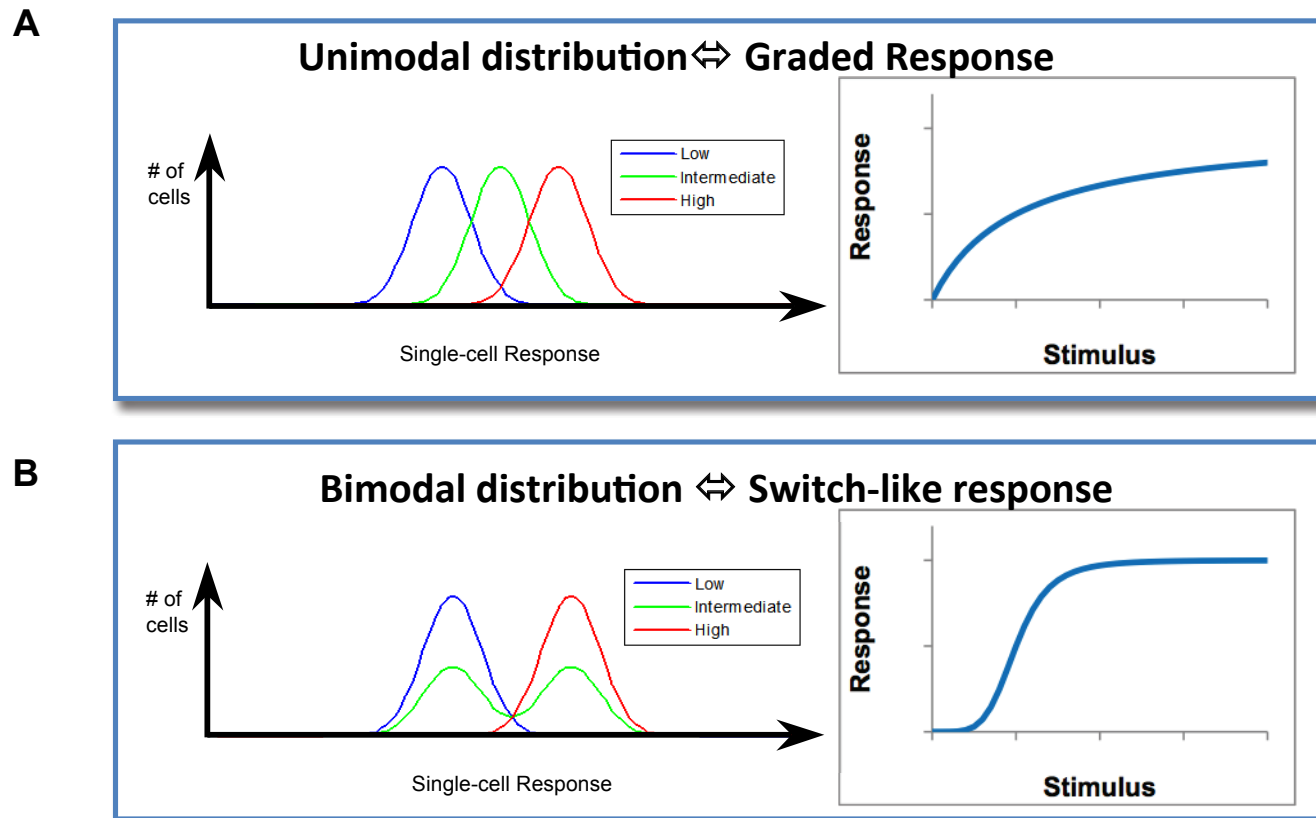
**Figure S7.** Torin 1-induced autophagy in L929 cells. Cells were treated with 200 nM Torin 1. Representative GFP-LC3 images and the corresponding segmentation results are shown for cells that are (A) untreated, (B) treated for 9 h, and (C) treated for 24 h. Each color in the segmented image represents puncta from a single cell. (D) The distributions of autophagosome scores at 0, 9 and 24 h. All distributions are unimodal.

## Figure S8. Torin 1-induced autophagy in HeLa cells



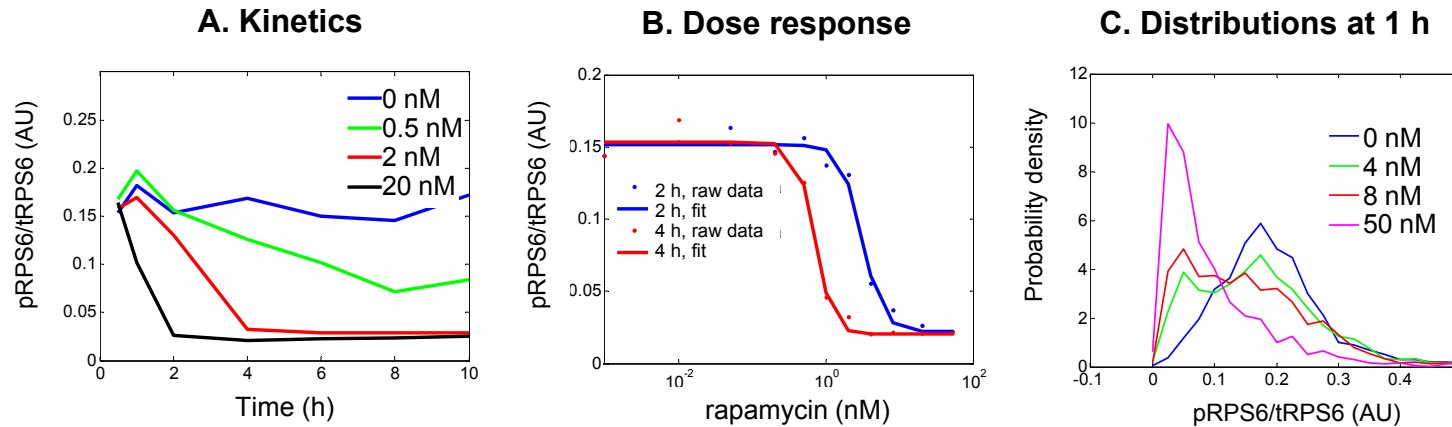
**Figure S8.** Torin 1-induced autophagy in HeLa cells. **(A)** Untreated control. **(B)** Cells were treated with 200 nM Torin 1 for 24 h. Images on the top are GFP-LC3, and the bottom images are corresponding segmented images. Note each color represents puncta from a single cell. **(C)** Mean autophagosome scores for control and 200 nM Torin 1-treated cells at 24 h. Error bars are standard error;  $n \geq 35$ .

## Figure S9. Graded and switch-like responses



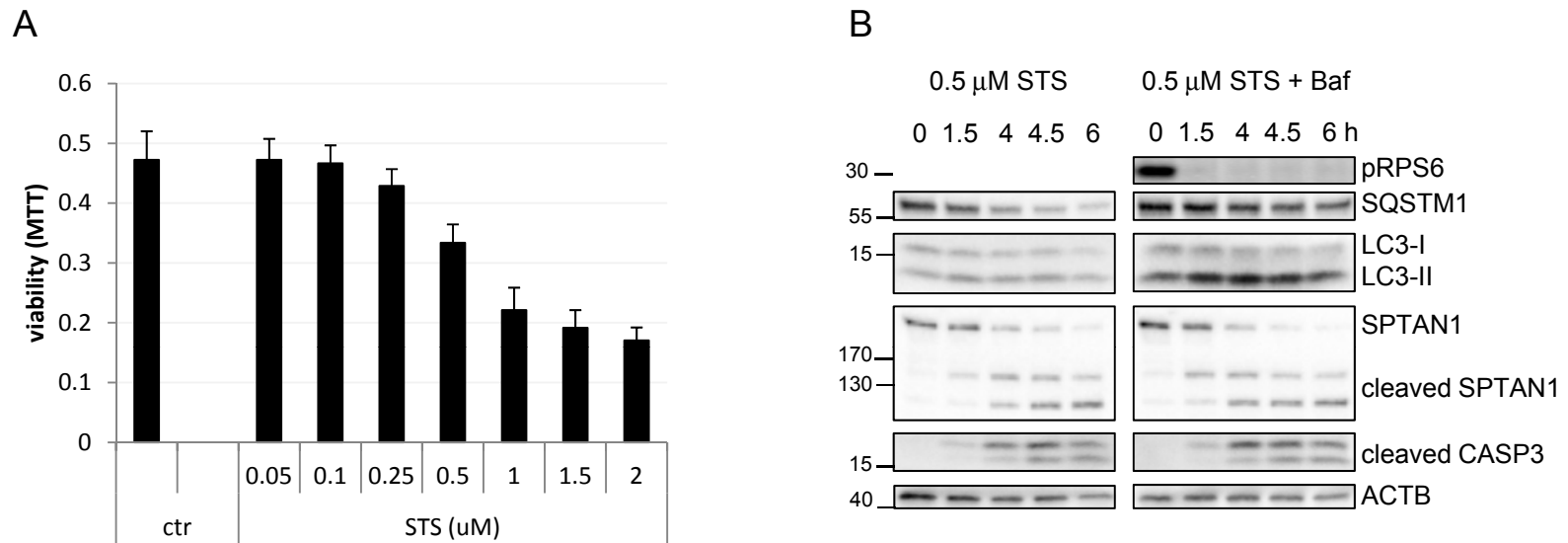
**Figure S9.** Cell-to-cell variation may be indicative of different types of signaling. The histograms illustrate the distribution of cell responses under low, intermediate and high stimuli. **(A)** If under the intermediate stimulus, all the cells respond similarly and form a unimodal distribution, this suggests the single-cell dose-response is graded (blue curve on the right, with abscissa in linear scale). **(B)** If under the intermediate stimulus, the cells make a binary decision and can only assume either low or high response state, the resultant distribution is bimodal, indicating the dose-response relationship is switch-like (abscissa in linear scale). Often the dose-response curves can be described by the Hill equation, and the switch-like response typically has much higher Hill coefficient, which reflects the slope of the dose-response curve. For more details please see refs. 4-5 and 10.

## Figure S10. Inhibition of RPS6 is switch-like



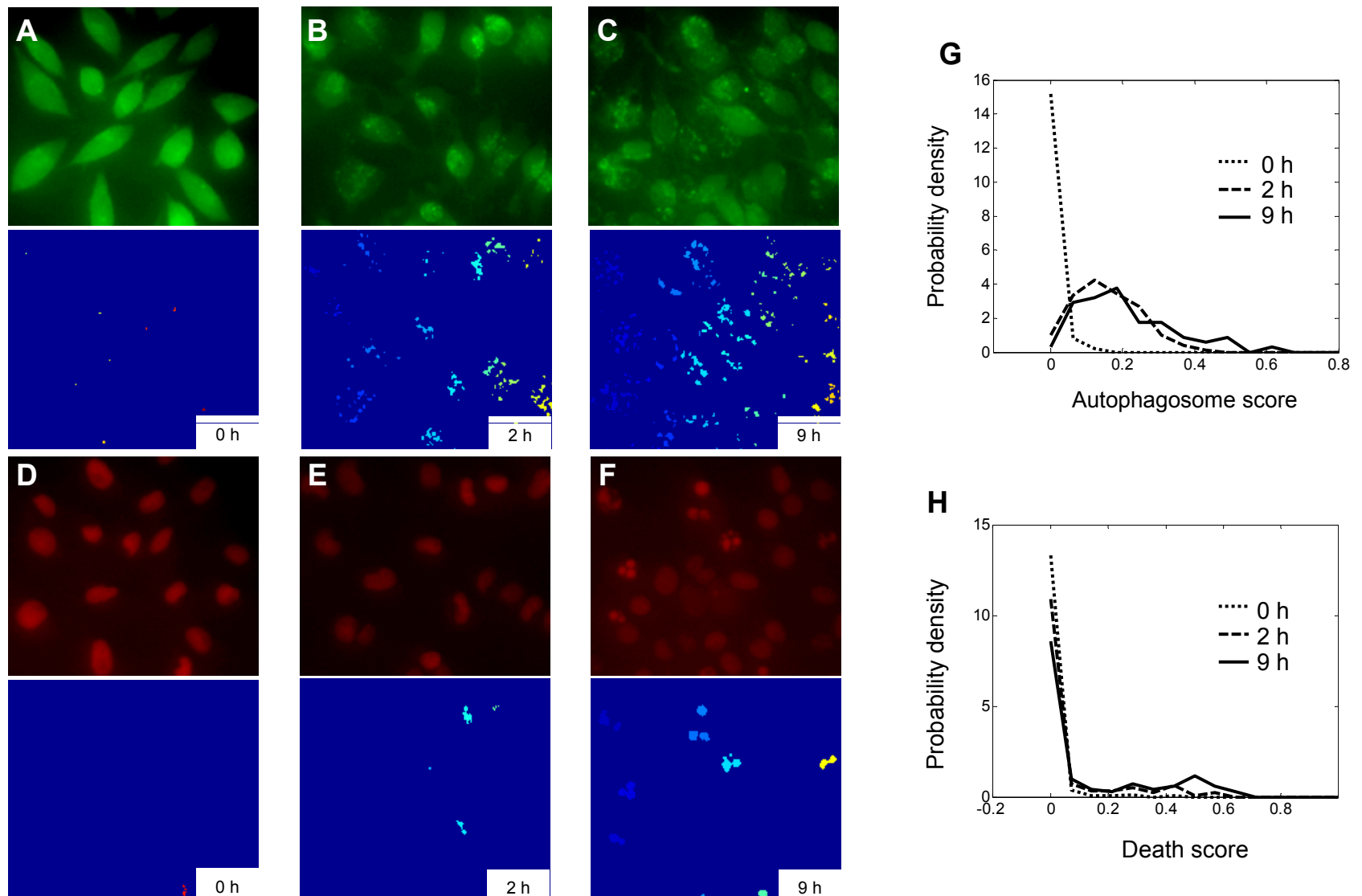
**Figure S10.** Kinetics and dose-response of inhibition of S6 Ribosomal protein (RPS6) phosphorylation by rapamycin, normalized by RPS6 expression (pRPS6/tRPS6). **(A)** Kinetics of population median. **(B)** Dose-response of population median. Data points are fitted by Hill's equation. **(C)** Distributions of pRPS6/tRPS6 at different concentrations of rapamycin. Note the distributions at intermediate doses (4 nM and 8 nM) are bimodal, indicating the inhibition of RPS6 activity is switch-like.

## Figure S11. Treatment with STS leads to induction of autophagy and apoptosis



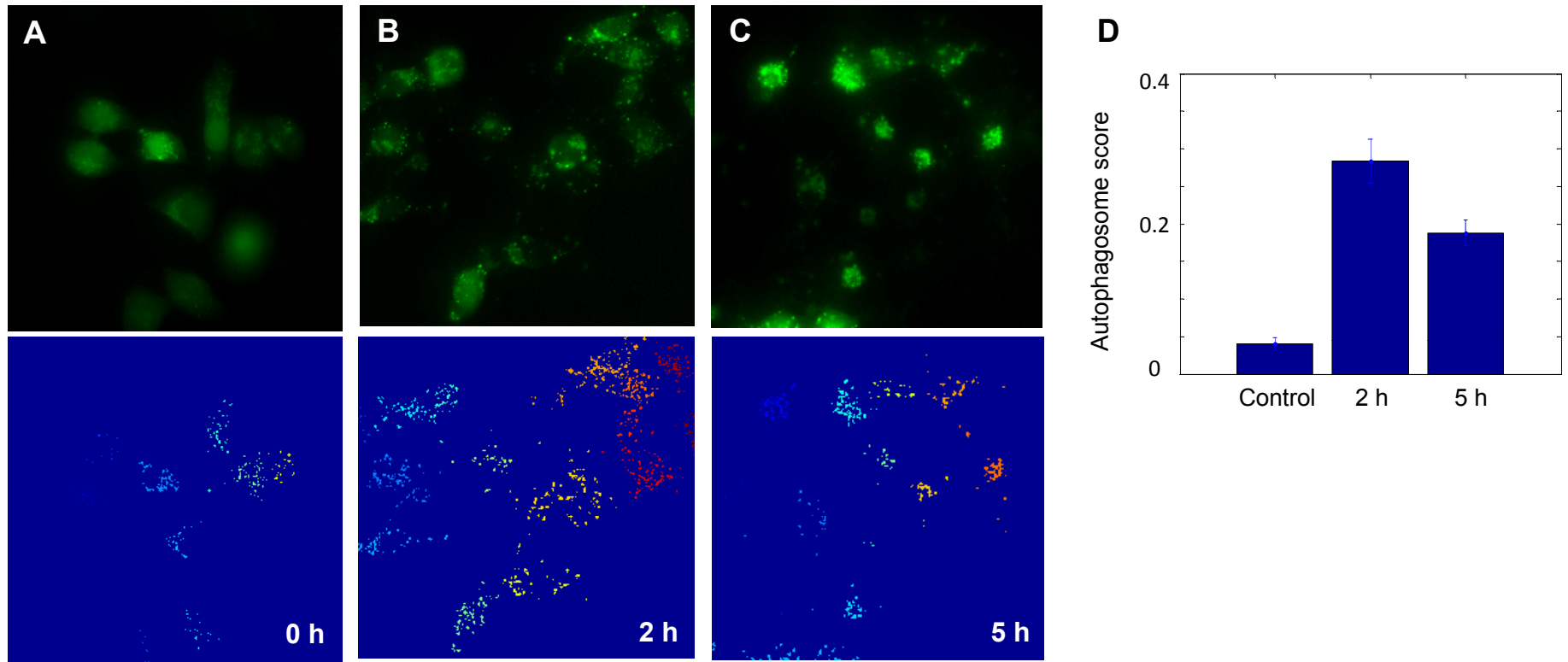
**Figure S11.** Treatment with STS leads to induction of autophagy and apoptosis. **(A)** Treatment with STS for 5 h decreased H4 cell viability in a dose-dependent manner as assessed by MTT assay. **(B)** Treatment of H4 cells with 0.5  $\mu$ M STS induced autophagy (accumulation of LC3-II and decreased levels of SQSTM1) and apoptotic cell death (decreased levels of full length SPTAN1, accumulation of cleaved SPTAN1 and active CASP3). Where indicated cells were treated with 100 nM Baf for 6 h prior to lysis.

Figure S12. STS-induced autophagy and apoptosis in L929 cells



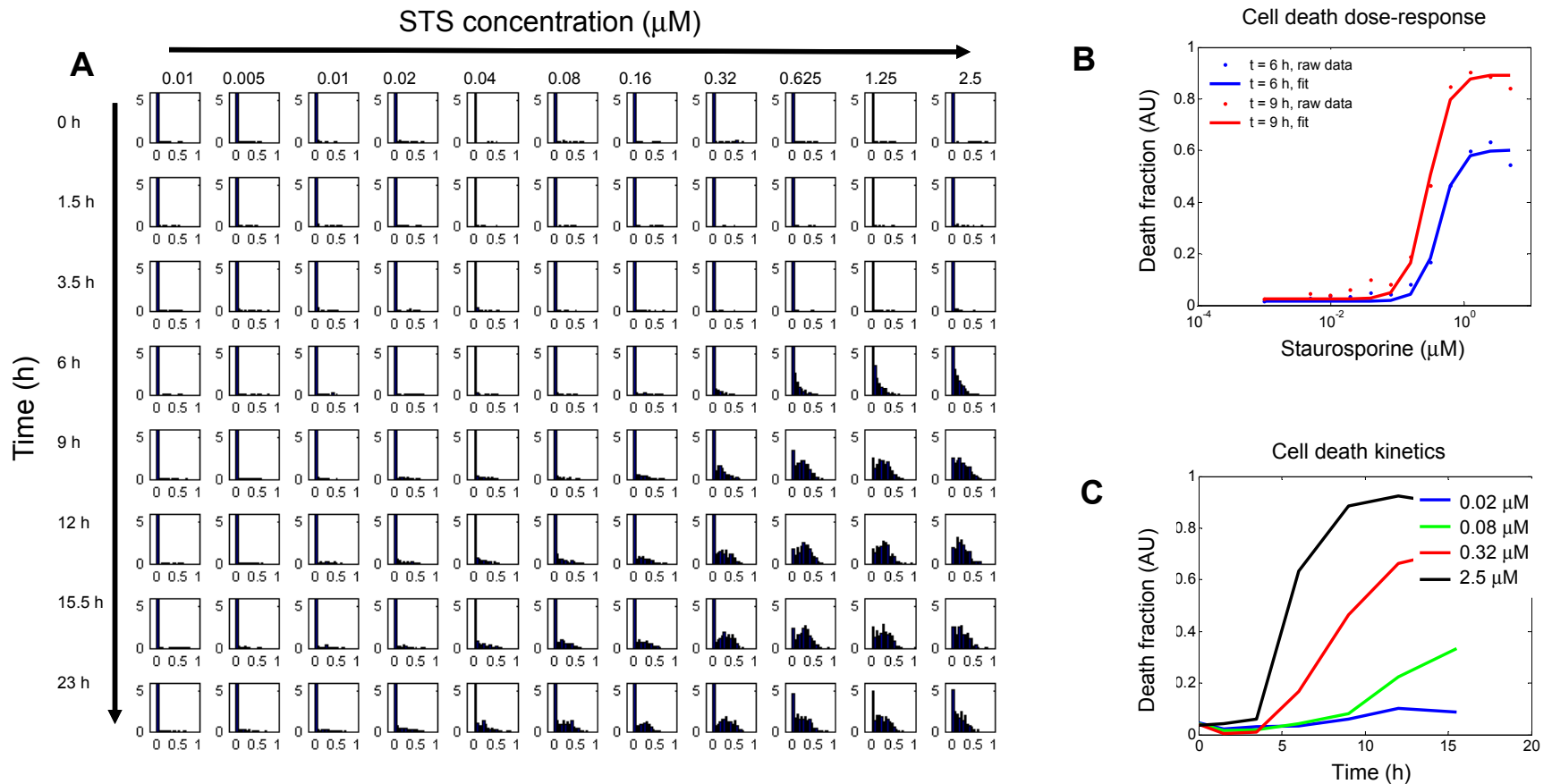
**Figure S12.** STS-induced autophagy and apoptosis in L929 cells. STS=2  $\mu$ M. GFP-LC3 images and their segmentation results are shown for cells that are (A) untreated, (B) treated for 2 h, and (C) treated for 9 h. H2B-RFP images and their segmentation results are shown in (D) untreated, (E) 2 h, and (F) 9 h. (G) Distributions of autophagy and (H) cell death are shown for the same time points.

Figure S13. STS-induced autophagy in HeLa cells



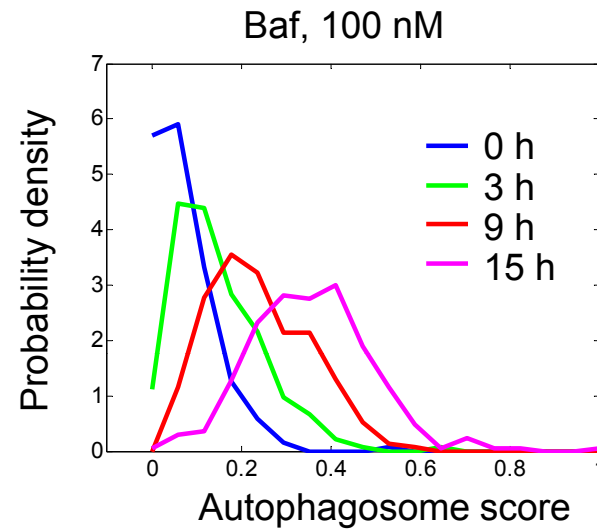
**Figure S13.** Detection of STS-induced autophagy in HeLa cells. (A) Untreated control. (B) 2  $\mu$ M STS for 2 h. (C) 2  $\mu$ M STS for 5 h. Images on the top and at the bottom are GFP-LC3 and segmentation results, respectively. Each color represents puncta from a single cell. (D) Autophagosome scores at indicated time points. Bars represent population means. Error bars are standard error,  $n \geq 30$ .

# Figure S14. Kinetics and dose-response of cell death in H4 cells after STS treatment



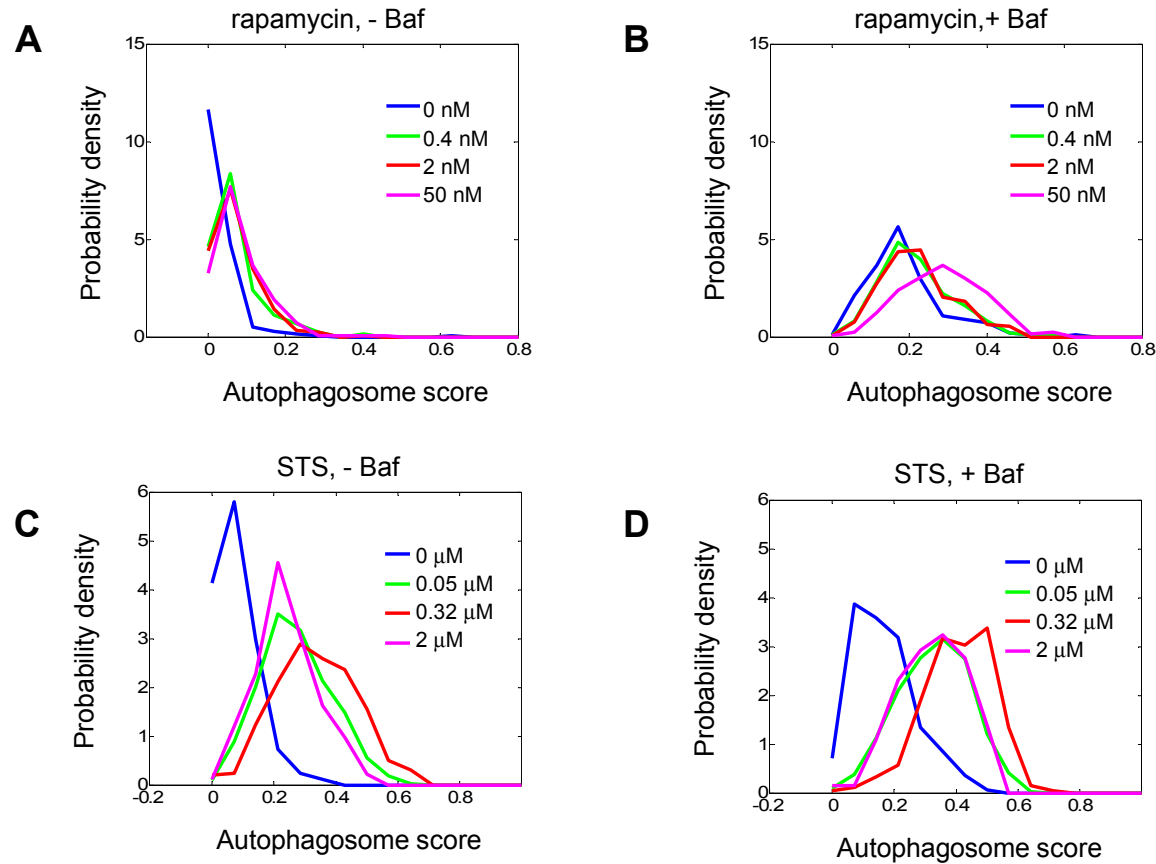
**Figure S14.** Kinetics and dose-response of cell death in H4 cells after STS treatment. LC3-H2B cells were treated with indicated doses of STS for different time. **(A)** Distributions of cell death scores as function of time and STS concentration. In the individual tiles, the X-axis is cell death score, and the Y-axis is probability density. **(B)** Dose response of fraction of cell death, fitted by the Hill equation. **(C)** Kinetics of fraction of cell death.

Figure S15. Distribution of autophagosome scores following inhibition of lysosomal degradation



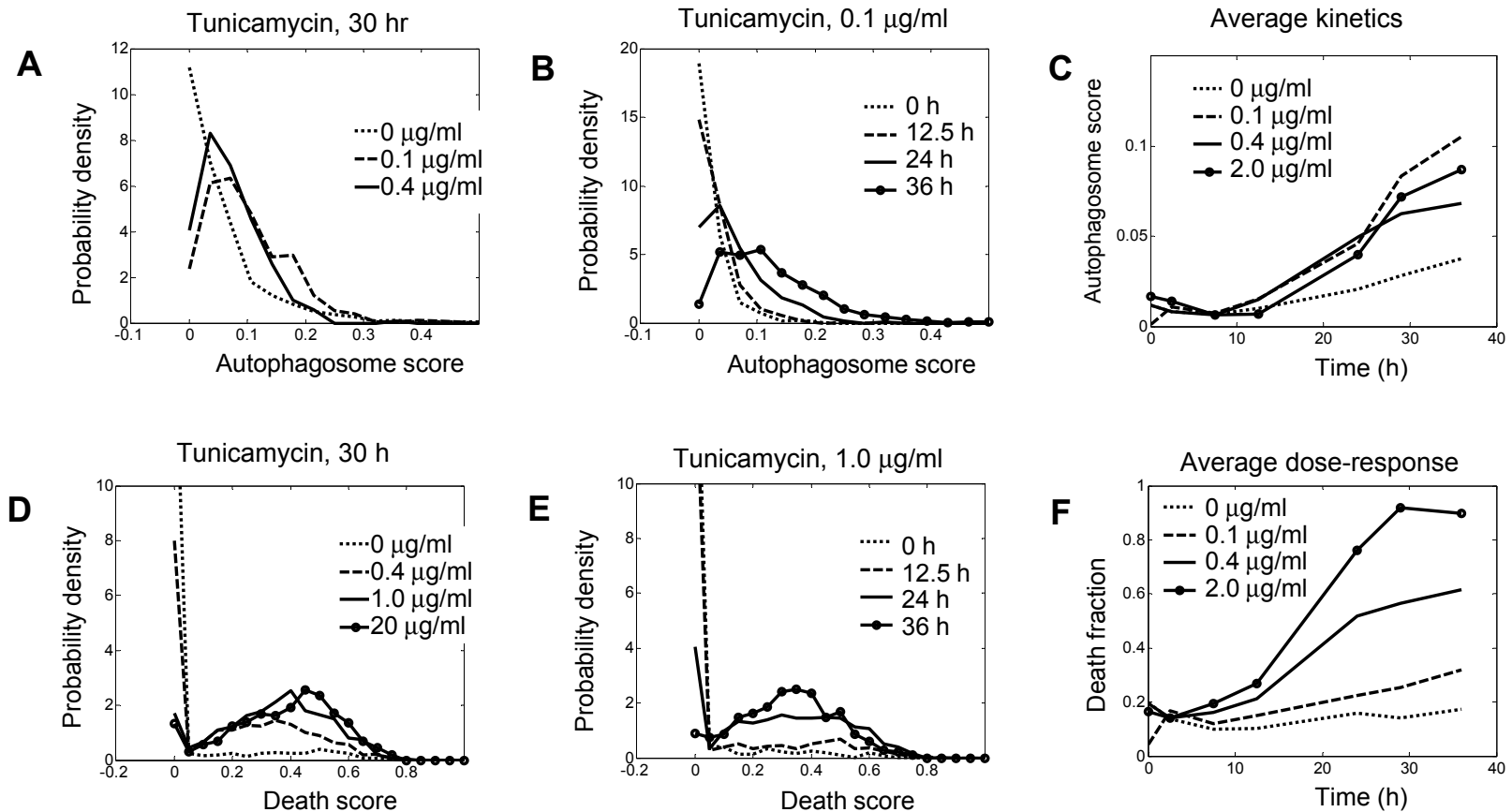
**Figure S15.** Distribution of autophagosome scores following inhibition of lysosomal degradation. H4 cells were treated with 100 nM Baf for indicated time periods. Note that the peak shifts with time and no apparent bimodality is discerned.

Figure S16. Effects of inhibition of lysosomal degradation on rapamycin- and STS- induced autophagy dynamics



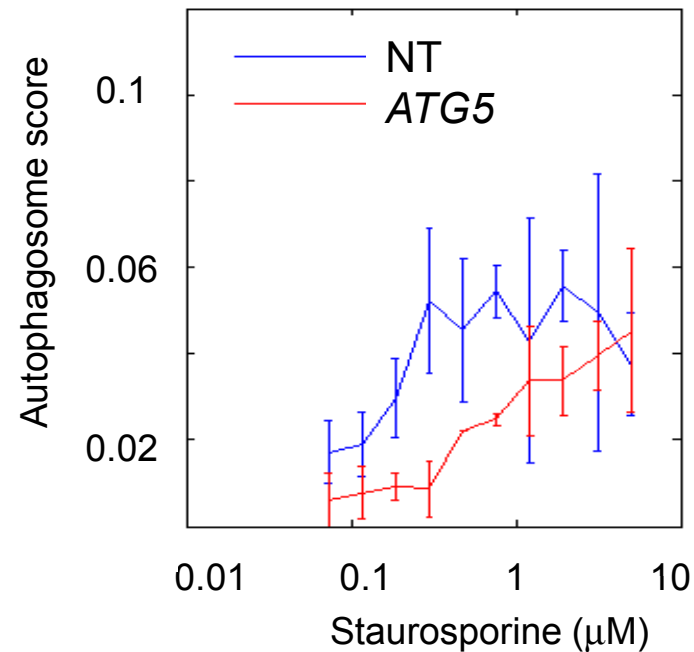
**Figure S16.** Effects of inhibition of lysosomal degradation on rapamycin- and STS- induced autophagy dynamics. **(A,B)** rapamycin-induced autophagy response at 7 h. **(A)** without Baf, **(B)** + 100 nM of Baf. **(C,D)** STS-induced autophagy response at 4 h. **(C)** without Baf, **(D)** + 100 nM of Baf.

Figure S17. Tunicamycin-induced autophagy and apoptosis in H4 cells



**Figure S17.** Tunicamycin-induced autophagy and apoptosis in H4 cells. **(A)** Dose-response of autophagosome score distributions at 30 h. **(B)** Kinetics of autophagosome score distributions, induced by 0.1 mg/ml of tunicamycin. **(C)** Kinetics of population median of autophagosome score. **(D)** Dose-response of death score distributions at 30 h. **(E)** Kinetics of death score distributions, induced by 1.0 mg/ml of tunicamycin. **(F)** Kinetics of population fraction of cell death.

Figure S18. Induction of autophagy by STS is suppressed by *ATG5* knockdown



**Figure S18.** Induction of autophagy by STS is suppressed by *ATG5* knockdown. H4 cells were transfected with siRNA against *ATG5* or a non-targeting siRNA control (NT) for 72 h. Dose response of autophagy 4 h following STS treatment of H4-GFP-LC3 cells is shown. Experiments were performed in 384-well plates in triplicate. Error bars are standard deviations between wells.